Unprecedented kinetic inertness for a Mn2+-bispidine chelate: a novel structural entry for Mn2+-based imaging agents

Daouda Ndiaye, Maryame Sy, Agnès Pallier, Sandra Même, Isidro de Silva, S. Lacerda, Aline M. Nonat, Loic Charbonniere, Éva Tóth

Unprecedented kinetic inertness for a Mn^{2+}-bispidine chelate: a novel structural entry for Mn^{2+}-based imaging agents

Daouda Ndiaye,[a] Maryame Sy,[b] Agnès Pallier,[a] Sandra Même,[a] Isidro de Silva,[c] Sara Lacerda,[a] Aline M. Nonat,[b] Loïc J. Charbonnière*[b] and Éva Tóth*[a]

[a] D. Ndiaye, A. Pallier, Dr. S. Même, Dr. S. Lacerda, Dr. É. Tóth
Centre de Biophyisique Moléculaire, CNRS UPR 4301, Université d'Orléans
rue Charles Sadron, 45071 Orléans, France
E-mail: eva.jakabtoth@cnrs-orleans.fr
[b] M. Sy, Dr. A. M. Nonat, Dr. L. J. Charbonnière
Equipe de Synthèse Pour l'Analyse
Université de Strasbourg, CNRS, IPHC UMR 7178
F-67000 Strasbourg, France
E-mail : L.Charbonn@unistra.fr
[c] I. da Silva
CEMHTI, CNRS UPR3079, Université d'Orléans
F-45071 Orléans 2, France

Supporting information for this article is given via a link at the end of the document.((Please delete this text if not appropriate))

Abstract: The search for more biocompatible alternatives to Gd^{3+}-based MRI agents, and the interest in ^{52}Mn for PET imaging call for ligands that form inert Mn^{2+} chelates. Given the labile nature of Mn^{2+}, high inertness is challenging to achieve. The strongly preorganized structure of the 2,4-pyridyl-disubstituted bispidol ligand L_1 endows its Mn^{2+} complex with exceptional kinetic inertness. Indeed, MnL_1 did not show any dissociation for 140 days in the presence of 50 eq. of Zn^{2+} (37°C, pH 6), while recently reported potential MRI agents MnPyC3A and MnPC2A-EA have dissociation half-lives of 0.285 h and 54.4 h under similar conditions. In addition, the relaxivity of MnL_1 (4.28 $mM^{-1}s^{-1}$ at 25°C, 20 MHz) is remarkable for a monohydrated, small Mn^{2+} chelate. *In vivo* MRI experiments in mice and determination of the tissue Mn content evidence rapid renal clearance of MnL_1. Additionally, L_1 could be radiolabeled with ^{52}Mn and the complex revealed good stability in biological media.

Introduction

The high diagnostic value of contrast agents makes them indispensable for many Magnetic Resonance Imaging protocols. For 35 years now, Gd-complexes have been used in millions of human examinations and considered among the safest diagnostic drugs. However, the recent emergence of nephrogenic systemic fibrosis and its causal link to Gd-exposure, as well as the evidence on brain and bone accumulation of Gd have alerted the medical community.[1] In response to these safety concerns, some of the linear Gd^{3+} chelates have been recently withdrawn and the use of others has been restricted. In this context, the replacement of Gd^{3+} with more biocompatible, safer paramagnetic metal ions has become a major objective.

Being an essential metal ion, as well as a good relaxation agent due to its five unpaired electrons (in the high spin state), slow electron spin relaxation and fast water exchange, Mn^{2+} is an obvious alternative.[2] Indeed, recent years have witnessed increasing interest in Mn^{2+} complexes as potential MRI agents.[3] In addition, manganese has a positron-emitting radioisotope, ^{52}Mn, with interesting decay properties for Positron Emission Tomography (PET) ($t_{1/2}$ = 5.6 d, max. β^+-energy: 575 keV). Given its low β^+ decay intensity (29.6%), PET resolution as good as 1.2 mm could be achieved which is particularly important in small animal imaging.[4] The long $t_{1/2}$ makes ^{52}Mn particularly adapted to image slow biological processes. Altogether, Mn^{2+} is the unique metal ion to offer detection capabilities in both MRI and PET.[5]

Thermodynamically stable and kinetically inert complexation of Mn^{2+} is indispensable to avoid *in vivo* release of the free metal ion, which could potentially cause toxicity during MRI where large contrast agent quantities are needed, or lead to off-target signals in PET examinations. In addition, for good MRI efficiency, the complex should contain at least one inner sphere water molecule. However, the lower charge (with respect to Gd^{3+}) and the lack of ligand-field stabilization energy for the high-spin d^5 electron configuration are not favorable to achieve high thermodynamic stability.

The highly labile nature of Mn^{2+} sets an even more difficult challenge to meet. Generally, ligand rigidity and preorganization promote kinetic inertness, and indeed, the most promising Mn^{2+} complexes are based on rigidified linear or macrocyclic chelators (Scheme 1). For instance, the *trans*-1,2-cyclohexylene backbone and the pyridine function ensure rigidity and are essential structural elements to provide slow dissociation of the MnPyC3A chelate (Scheme 1), a potential Mn^{2+}-based agent which has successfully passed to *in vivo* experiments.[3a, 6] Among macrocyclic chelates, the non-hydrated MnDOTA was reported to have high inertness,[7] while the monohydrated [Mn(cisDO2A)] was found already ~20-fold more labile (dissociation half-lives, $t_{1/2}$, estimated to 1061 h and 48 h, respectively, at pH 7.4).[8]

Recently, derivatives of the pyridine-containing pyclen macrocycle were found to form stable and very inert Mn^{2+} chelates.[3c] With $t_{1/2}$ = 8×10^3 h estimated for pH 7.4, the Mn(PC2A-EA) complex bearing an ethyleneamine pendant arm and proposed as a pH-sensitive agent, has the highest resistance to dissociation ever reported for a monohydrated Mn^{2+} complex. Nevertheless, this dissociation half-life remains a million times below the value for GdDOTA ($t_{1/2}$ =2.7 × 10^9 h, pH 7.4 and 25 °C).

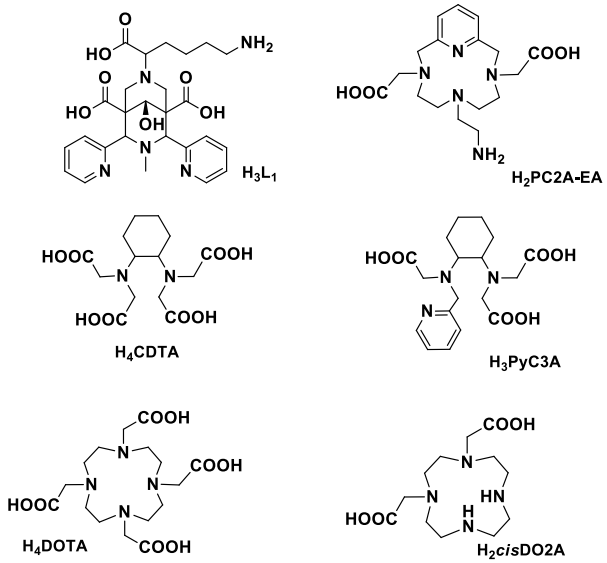

Scheme 1. Ligands discussed.

In the aim of substantially improving the kinetic inertness of Mn^{2+} chelates while ensuring good relaxation properties and water solubility, we are exploring bispidine (3,7-diazabicyclo[3.3.1]nonane) derivatives. Bispidine-type ligands represent a versatile platform in coordination chemistry.[9] Pendant arms with varying coordinating functions can be attached in different positions to the bicyclic amine core in order to tune the coordination properties for metal ions of various sizes, coordination numbers or coordination geometries. Depending on the substituents, the ligand can adopt different conformations and configurations.[10] Among those, the chair-chair conformer is best suited for stable metal coordination and thanks to its exceptionally preorganized structure, bispidine derivatives tend to form very inert complexes. Bispidine complexes have been investigated with a large variety of metal ions and for different applications. Concerning Mn^{2+}, the very scarce reports involve pyridine derivative bispidine ligands and are restricted to studies in the solid state or in non-aqueous solvents.[11]

We hypothesized that the 2,4-pyridyl-disubstituted bispidol derivative L_1 bearing one methylene carboxylic acid (Scheme 1) could be a good chelator for Mn^{2+}. First, the very rigid bispidine scaffold can endow MnL_1 with high kinetic inertness. The ligand is expected to coordinate in a five-dentate manner, involving two pyridine and two bispidine nitrogens as well as the methylene carboxylate. This leaves one coordination site for a hydration water, important for MRI application. The non-coordinating pending carboxylates might additionally create a second sphere contribution and increase proton relaxivity. Finally, L_1 can be readily functionalized for biological targeting *via* the lysine terminal amine. This scaffold has been previously investigated for the complexation of $^{64/67}Cu^{2+}$[12] and $^{68}Ga^{3+}$.[13] A three dimensional representation of the putative structure of the MnL_1 complex is shown in Scheme 2.

We evidence here that despite a moderate thermodynamic stability, MnL_1 has a resistance to acid catalyzed dissociation and transmetalation which is unprecedented for a Mn^{2+} chelate. In addition, the relaxation efficiency of the complex was assessed by a combined ^{17}O NMR and NMRD study. The complex was injected into mice and its biodistribution and pharmacokinetics were monitored by MRI. Finally, the ^{52}Mn radiolabelling of L_1 was explored and the stability of the radiocomplex was investigated.

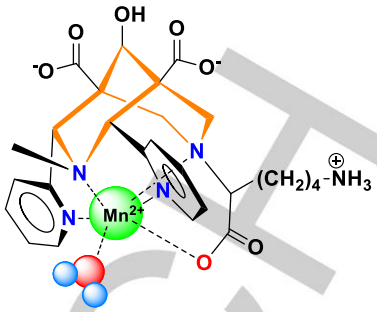

Scheme 2. Three dimensional representation of the putative structure of MnL_1.

Results and Discussion

L_1 was synthesized in 4 steps as previously reported.[12]

Thermodynamic stability and kinetic inertness of MnL_1

Ligand protonation constants were obtained by pH potentiometry and are reported in Table 1. By analogy to other bispidine ligands,[14] we attributed the first protonation constant to one of the tertiary amine groups, while the other amine of the bispidine skeleton remains likely unprotonated in the chair-chair conformation.[14b] Further protonation steps supposedly occur on the lysine amine ($\log K_{H2}$ = 10.31, typical of the lysine ε amine protonation constant)[15] and then on the three carboxylates, while the pyridine nitrogens are not protonated above pH 2. Thermodynamic stability constants of MnL_1 and ZnL_1 were assessed by pH potentiometry (Table 1). In the case of Mn^{2+}, slow complex formation prevented direct titration; therefore, batch samples were prepared (Fig. S1). MnL_1 is three orders of magnitude less stable than ZnL_1, in accordance with the Irving–Williams series. Figure 1 depicts the species distribution for MnL_1 as a function of pH, supported by the pH-dependent relaxivities. Protonated complexes form with both Zn^{2+} and Mn^{2+}; the first protonation constants are practically identical to $\log K_{H2}$ of the ligand and correspond to the protonation of the non-coordinating lysine amine. The similarity between the second protonation constant of the ligand and $\log K_{MnHL}$ or $\log K_{ZnHL}$ further supports the attribution of the ligand protonation steps. At physiological pH, this species protonated on the lysine ε amine is the only complex present.

Table 1. Ligand protonation constants, stability constants of ML complexes and pMn values. Values in parenthesis correspond to one standard deviation.

	L_1	PyC3A[3a]	trans-CDTA[16]	PC2A-EA[6]
$\log K_{H1}$	11.44(1)	10.16	9.54	11.34
$\log K_{H2}$	10.31(2)	6.39	5.97	8.93
$\log K_{H3}$	4.71(5)	3.13	3.60	6.91
$\log K_{H4}$	2.76(5)	-	2.52	1.97
$\log K_{H5}$	2.22(4)	-	1.46	-

$\Sigma\log K_{Hi}$	31.5	19.68	23.09	18.25
$\log K_{MnL}$	12.21(5)	14.14	14.32	19.01
$\log K_{MnHL}$	10.42(3)	2.43	2.90	6.88
$\log K_{MnH2L}$	3.87(4)	-	1.89	2.50
$\log K_{ZnL}$	15.59(3)	-	16.75	-
$\log K_{ZnHL}$	10.33(2)	-	2.57	-
$\log K_{ZnH2L}$	3.28(1)	-	-	-
pMn[a]	6.65	8.17	8.68	9.27

[a] pMn calculated for $c_{Mn} = c_{lig} = 10^{-5}$ M; pH 7.4

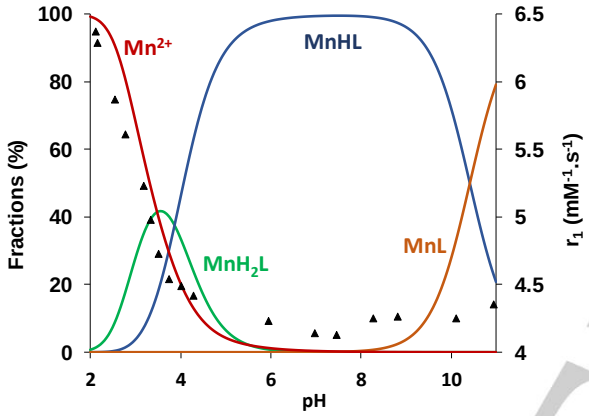

Figure 1. Species distribution curves calculated for MnL_1 (1 mM) and pH-dependent relaxivities (▲) measured at 25°C, 60 MHz.

The stability of MnL_1 is relatively modest, as shown by the pMn value of 6.65 calculated for 10^{-5} M Mn^{2+} and L_1 concentration and pH 7.4 (Table 1). Nevertheless, once the chelate is formed, it has an exceptional resistance to dissociation. Kinetic inertness of metal complexes is typically assessed by transmetalation experiments with endogenously available metal ions, such as Zn^{2+}, which is present at ~10 μM concentration in the blood and represents the most abundant potential competitor of Mn^{2+}. Different transmetalation protocols have been reported for Mn^{2+} complexes, some allowing a simple comparison of the kinetic inertness under given conditions, others giving also access to the underlying dissociation mechanisms. We followed transmetalation in the presence of 10 or 50 equivalents of Zn^{2+}, at pH 6 (50 mM MES buffer), 37°C, in a similar way to that proposed by Caravan et al.[3a] At either of the Zn^{2+} concentrations, MnL_1 did not show any relaxivity change for the 140 days of observation (Fig. 2). Under similar conditions (37°C, pH 6.0, 25 Zn^{2+} equivalents), dissociation half-lives, $t_{1/2}$, of 0.285 h and 54.4 h have been reported respectively for MnPyC3A[3a] and MnPC2A-EA[3c], two reference compounds considered as potential MRI probes with good kinetic inertness. Analogous experiments have been carried out at more acidic pH values as well (pH 3.1-6.0, 50 equivalents Zn^{2+}, 37 °C; Fig. 2). Under these pseudo-first order conditions, the dissociation rate constant, k_{obs}, has been determined, and the estimated transmetalation half-lives vary between 22.7 h at pH 3.13 and 130 days at pH 5.07.

The inertness of MnL_1 was also assessed in highly acidic solutions where the dissociation is much faster (0.01-1.0 M HCl, 25°C; Fig. 3). The dissociation rate constants, k_{obs}, show a second order dependence on the proton concentration and could be fitted to Eq. 1.

$$k_{obs} = k_0 + k_1[H^+] + k_2[H^+]^2 \quad \text{(Eq. 1)}$$

The fit resulted in k_1 = (1.6±0.1)×10^{-3} s^{-1} M^{-1} and k_2 = (5.0±0.1)×10^{-4} s^{-1} M^{-2}, while k_0 was fixed to 0, otherwise the fit yielded a negative value with a large error (-3.5±2)×10^{-5} s^{-1}. We should note that the k_{obs} values determined above in the Zn^{2+} transmetalation study in the pH 3.1-5.1 interval also show a second order dependence on [H^+] (Fig. S2), with k_1 = (2.2±0.2)×10^{-3} s^{-1} M^{-1}, in the same order of magnitude as the one above. This rate constant, characterizing the proton assisted dissociation pathway, is two orders of magnitude lower than that reported for MnPC2A-EA which is the most inert hydrated Mn^{2+} chelate reported so far.[3c] At this point, it is difficult to extrapolate the dissociation half-life of the complex for physiological conditions, and in particular, more data are needed to describe the role of metal-assisted dissociation processes in the overall dissociation. These studies are in progress, but they are long due to the extremely low dissociation rates. Nevertheless, we can conclude that the rigid and preorganized bispidine skeleton provides very high kinetic inertness, unprecedented for a Mn^{2+} chelate.

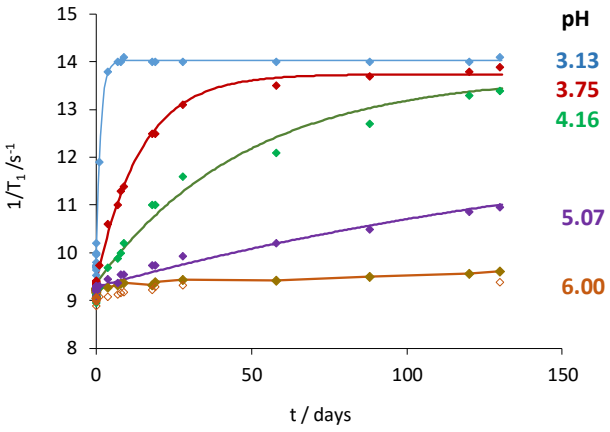

Figure 2. Time-dependent variation of the longitudinal proton relaxation rates in a 1 mM MnL_1 solution at 37°C and 60 MHz, 0.1 M KCl, in the presence of 50 equivalents of Zn^{2+}. Empty symbols at pH 6.00 correspond to 10 equivalents of Zn^{2+}. The curves represent the fit of the experimental data to yield the observed rate constants, k_{obs}.

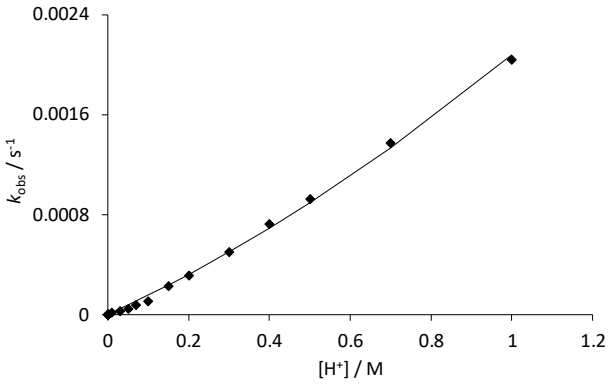

Figure 3. Pseudo-first order rate constants determined for the dissociation of MnL_1 in acidic solutions. The curve corresponds to the fit of the experimental data to Eq. (1) as explained in the text.

Relaxation properties of MnL_1

Proton relaxivities have been recorded for MnL_1 as a function of the magnetic field, at 25 and 37°C, in water (pH 7) and in human serum (Figs. 4a and S3). The NMRD data were complemented by variable temperature ^{17}O relaxation rate measurements (Fig. 4b) which give access to the hydration number and the water exchange parameters. The relaxivity is remarkably high for a Mn^{2+} complex (r_1 = 4.28 $mM^{-1}s^{-1}$ and 3.37 $mM^{-1}s^{-1}$ at 25°C and 37°C, respectively, 20 MHz, pH 7 in water). In comparison, relaxivities of 3.3 and 2.5 $mM^{-1}s^{-1}$ (20 MHz, 25 and 37 °C) and 3.52 $mM^{-1}s^{-1}$ (20 MHz, 25°C) were reported for the monohydrated complexes MnPCy3A and MnPC2A-EA. One hydration water molecule is confirmed for MnL_1 from the temperature-dependent ^{17}O transverse relaxation rates using the method of Gale et al. (q = 0.85; Fig. S4).[17]

The temperature-dependent transverse ^{17}O relaxation rates and the NMRD profiles have been analysed in the frame of the Solomon-Bloembergen-Morgan theory to determine the parameters describing water exchange and rotational dynamics. The fit yielded k_{ex}^{298} = (5.1±0.7)×10^7 s^{-1} and $\Delta H^{\ddagger}$ = 10.6 kJ/mol for the rate and the activation enthalpy of the water exchange. The water exchange rate is similar to that reported for MnPyC3A (k_{ex}^{298} = 5.4×10^7 s^{-1})[3a] while it is about ten times lower than k_{ex}^{298} on MnEDTA (k_{ex}^{298} = 47×10^7 s^{-1}).[18] The bispidine MnL_1 chelate is structurally very different from other previously studied Mn^{2+} complexes, and the reason for this relatively slow water exchange is difficult to identify. Nevertheless, this exchange rate remains high enough not to limit proton relaxivity. The rotational correlation time, τ_R^{298} = (100±2) ps, is higher than the values reported for small molecular weight Mn^{2+} complexes (e.g. 56 ps for MnEDTA).[19] This might reflect that τ_R is overestimated due to second sphere contribution to relaxivity from the non-coordinating carboxylates. Therefore, we also performed the analysis of the NMRD data by including an additional contribution from a second sphere relaxation mechanism to the overall relaxivity. To describe this second sphere mechanism, we assumed two 2nd sphere water molecules (with an estimated Mn-H proton distance of 3.2 Å, 50 ps residence time and an activation enthalpy of 10 kJ/mol, based on previous simulations on Gd^{3+} complexes; see Fig. S5 and ESI for all details).[20] This resulted in a rotational correlation time, τ_R^{298} = (72±4) ps which seems more reasonable on the basis of the molecular weight of the complex. This is obviously not a firm proof of a second sphere relaxivity contribution; nevertheless, it is evident that the relaxivities measured tend to be higher than the typical values reported for monohydrated Mn^{2+} chelates.

The relaxivities remain identical in the presence of up to 50 equivalents of citrate, carbonate and phosphate (Fig. S6). They increase to 6.46 and 5.12 $mM^{-1}s^{-1}$ in human serum at 25 and 37 °C, respectively (20 MHz, Fig. 4a), a tendency similar to that observed for instance for MnPyC3A and attributed to low affinity binding to serum proteins.

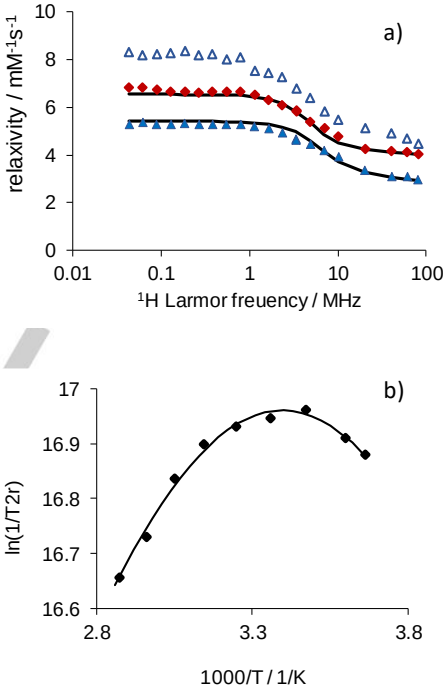

Figure 4. a) Proton relaxivities of MnL_1 measured in water at 25°C (♦) and 37 °C (▲) and in human serum at 37 °C (Δ), and b) reduced transverse ^{17}O relaxation rates (9.4 T). The lines represent the simultaneous fit of the experimental points as explained in the text.

^{52}Mn radiolabeling of L_1

The need for long-lived β^+-emitting isotopes and the emergence of a combined PET-MRI technology have recently promoted an increasing interest in the production and complexation of ^{52}Mn. We have produced and purified ^{52}Mn at the cyclotron of the Orléans CNRS campus (see ESI for details). ^{52}Mn was recovered as $^{52}MnCl_2$ solution after purification through 2 anion exchange resin AG© 1-X8 columns. The radiolabelling of L_1 was tested under different conditions of pH, temperature and ^{52}Mn:L_1 ratio. The radiolabelling reactions were followed by radioTLC at 5, 15, 30 and 60 min. All reactions were performed in presence of ascorbic acid to prevent any oxidation reaction. Optimized reaction conditions were obtained for pH 7, 70 °C, 1h, achieving 99% labelling yield. $^{52}MnL_1$ is highly hydrophilic with a log$P$ = -1.96±0.06, which falls within the range reported for other Mn complexes, e.g. MnDPDP or Mn(EDTA-BTA) with log$P$ values of -3.07 and -1.84, respectively.[21] The *in vitro* stability of the radiocomplex was assessed in different media at pH 7.4 (water, PBS and saline (0.9% NaCl)) and in the presence of 0.6 mM

HSA (Fig. 5), revealing its stability in all media up to 18h, and a slightly lower to moderate stability at 24h.

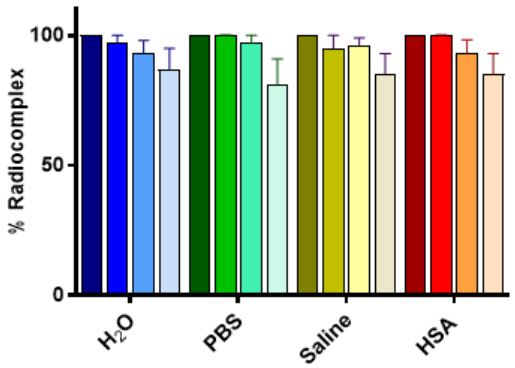

Figure 5. *In vitro* stability of $^{52}MnL_1$ in different media at pH 7.4 (water, PBS and saline (0.9% NaCl)) and in the presence of 0.6 mM HSA, at different time points: 0, 1, 18 and 24 h (darker to lighter colour, respectively).

MRI biodistribution and pharmacokinetics of MnL_1

To validate the potential *in vivo* use of MnL_1, we have evaluated the biodistribution in wild type mice by MRI at 7 T. The signal intensity of the main organs (kidney, liver, muscle, lung) and the aorta was followed during 1 h post intravenous injection (0.06 mmol/kg dose; Fig. S7). Figure 6 depicts normalized signal intensity for the analyzed organs. The highest signal intensity was reached around 4 min after injection. MnL_1 shows renal clearance and the uptake in the liver is limited. The estimated blood half-life is 21 min, typical of small molecules and similar to previously reported contrast agents.[3a, 22] This distribution profile was further confirmed by *ex vivo* ICP-OES measurements performed at the end of the MRI experiment. The data are compared to mice which did not receive any MnL_1 injection (control) where the Mn-levels measured correspond to endogenous Mn (Fig. 7; Table S1).

At 1.5 h post injection, higher Mn content is found in the kidneys and blood of injected mice. The blood uptake could be related to the low affinity binding of MnL_1 to blood proteins, as also observed by relaxivity measurements. Compared to the Mn tissue content reported for MnPyC3A at 24 h post injection, our complex shows lower liver and kidney uptake.[3a]

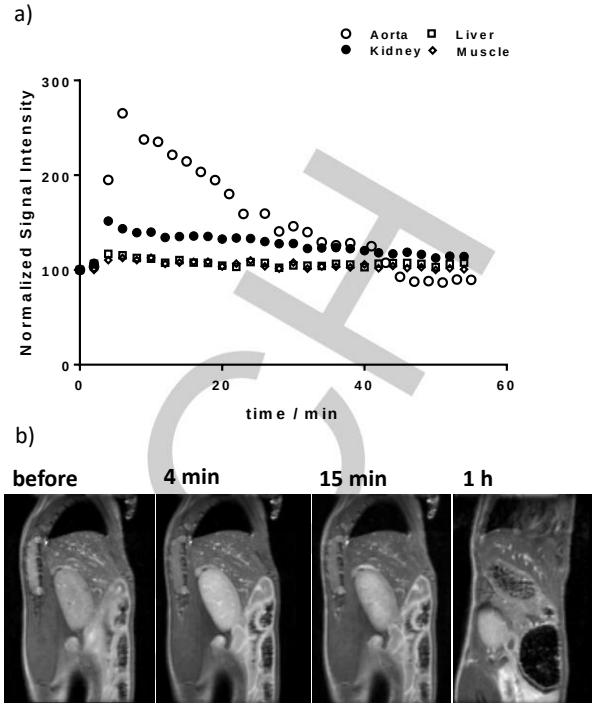

Figure 6. a) Normalized signal intensity in the kidney, muscle, liver and aorta plotted as a function of time. Measurements were performed every 2 minutes for 4 mice. Standard deviations are not presented for better readability. b) Sagittal T1-weighted MR images prior to injection and at 4, 15 min and 1 h post intravenous injection of 0.06 mmol/kg of MnL_1.

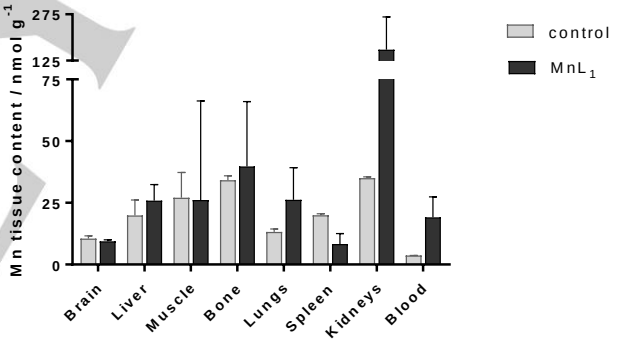

Figure 7. *Ex vivo* ICP-OES quantification of the Mn tissue content in the main organs and blood of control and injected mice with MnL_1 (1.5 h post injection). Data is presented in nmol/g tissue ± SD (n=3).

Conclusion

We demonstrate here that despite a relatively modest thermodynamic stability, the MnL_1 complex has an exceptional resistance to dissociation. At 37°C, pH 6.0 and in the presence of up to 50 equivalents of Zn^{2+}, MnL_1 remained intact and did not show any relaxivity change for at least 140 days. MnL_1 has one inner sphere water molecule. It has higher proton relaxivities than most monohydrated, small molecular weight Mn^{2+} chelates, which might be related to a second sphere relaxivity contribution induced by the non-coordinating carboxylates functions.

In vivo MRI experiments performed in mice indicated quick renal clearance, which was also supported by *ex vivo* ICP determination of the Mn tissue content in different organs. L_1 could be successfully labeled with ^{52}Mn and the radiocomplex has good stability in biological media. Based on these

preliminary radiolabeling experiments, the conjugation of the bifunctional ligand L_1 to biomolecules, such as antibodies can be envisaged. Indeed, for the imaging of such slowly circulating biomolecules, the long-lived ^{52}Mn PET isotope represents a clear advantage.

In summary, the bispidine-based L_1 chelator constitutes a very promising structural entry for the development of Mn-based imaging agents for MRI as well as for PET. Alternatively, this bispidine synthon can be also attractive for the design of combined PET-MRI probes. Such bimodal imaging applications based on Mn^{2+} might be interesting when the *in vivo* fate of the imaging probe is to be followed for a longer period of time. Most importantly, the L_1 ligand can provide excellent kinetic inertness which so far could not be achieved within the more traditional ligand families.

Experimental Section

Experimental details are described in detail in the Supporting Information.

Acknowledgements

The authors thank the French National Research Agency (grant ANR-18-CE18-0008) for funding. We thank Dr. Frederic Szeremeta and Quentin Mura for their assistance with MRI experiments and Louis Frealle with the ^{52}Mn production.

Keywords: manganese • contrast agent • MRI • ^{52}Mn • kinetic inertness

[1] aT. Grobner, *Nephrol. Dial. Transplant.* **2006**, *21*, 1104-1108; bE. Di Gregorio, G. Ferrauto, C. Furlan, S. Lanzardo, R. Nuzzi, E. Gianolio, S. Aime, *Invest. Radiol.* **2018**, *53*, 167-172.

[2] B. Drahoš, I. Lukeš, É. Tóth, *Eur. J. Inorg. Chem.* **2012**, *2012*, 1975-1986.

[3] aE. M. Gale, I. P. Atanasova, F. Blasi, I. Ay, P. Caravan, *J. Am. Chem. Soc.* **2015**, *137*, 15548-15557; bM. Botta, F. Carniato, D. Esteban-Gomez, C. Platas-Iglesias, L. Tei, *Future Med. Chem.* **2019**, *11*, 1461-1483; cR. Botár, E. Molnár, G. Trencsényi, J. Kiss, F. K. Kalman, G. Tircsó, *J. Am. Chem. Soc.* **2020**; dZ. Garda, E. Molnár, F. K. Kálmán, R. Botár, V. Nagy, Z. Baranyai, E. Brücher, Z. Kovács, I. Tóth, G. Tircsó, *Front. Chem.* **2018**, *6*, 14; eE. Molnar, N. Camus, V. Patinec, G. A. Rolla, M. Botta, G. Tircso, F. K. Kalman, T. Fodor, R. Tripier, C. Platas-Iglesias, *Inorg. Chem.* **2014**, *53*, 5136-5149; fA. Rodriguez-Rodriguez, Z. Garda, E. Ruscsak, D. Esteban-Gomez, A. de Blas, T. Rodriguez-Blas, L. M. P. Lima, M. Beyler, R. Tripier, G. Tircso, C. Platas-Iglesias, *Dalton Trans.* **2015**, *44*, 5017-5031; gC. Vanasschen, E. Molnar, G. Tircso, F. K. Kalman, E. Toth, M. Brandt, H. H. Coenen, B. Neumaier, *Inorg. Chem.* **2017**, *56*, 7746-7760.

[4] L. M. Carter, A. L. Kesner, E. C. Pratt, V. A. Sanders, A. V. F. Massicano, C. S. Cutler, S. E. Lapi, J. S. Lewis, *Mol. Imag. Biol.* **2020**, *22*, 73-84.

[5] C. M. Lewis, S. A. Graves, R. Hernandez, H. F. Valdovinos, T. E. Barnhart, W. Cai, M. E. Meyerand, R. J. Nickles, M. Suzuki, *Theranostics* **2015**, *5*, 227-239.

[6] D. J. Erstad, I. A. Ramsay, V. C. Jordan, M. Sojoodi, B. C. Fuchs, K. K. Tanabe, P. Caravan, E. M. Gale, *Invest. Radiol.* **2019**, *54*, 697-703.

[7] B. Drahos, V. Kubicek, C. S. Bonnet, P. Hermann, I. Lukes, E. Toth, *Dalton Trans.* **2011**, *40*, 1945-1951.

[8] Z. Garda, A. Forgács, Q. N. Do, F. K. Kálmán, S. Timári, Z. Baranyai, L. Tei, I. Tóth, Z. Kovács, G. Tircsó, *J. Inorg. Biochem.* **2016**, *163*, 206-213.

[9] aA. M. Nonat, A. Roux, M. Sy, L. J. Charbonniere, *Dalton Trans.* **2019**, *48*, 16476-16492; bP. Comba, M. Kerscher, W. Schiek, in *Progress in Inorganic Chemistry, Vol. 55* (Ed.: K. D. Karlin), **2007**, pp. 613-704; cP. Comba, M. Kerscher, K. Rueck, M. Starke, *Dalton Trans.* **2018**, *47*, 9202-9220.

[10] T. Legdali, A. Roux, C. Platas-Iglesias, F. Camerel, A. M. Nonat, L. J. Charbonniere, *J. Org. Chem.* **2012**, *77*, 11167-11176.

[11] aP. Comba, B. Kanellakopulos, C. Katsichtis, A. Lienke, H. Pritzkow, F. Rominger, *J. Chem. Soc.-Dalton Trans.* **1998**, 3997-4001; bP. Comba, H. Rudolf, H. Wadepohl, *Dalton Trans.* **2015**, *44*, 2724-2736; cP. Comba, M. Kerscher, M. Merz, V. Muller, H. Pritzkow, R. Remenyi, W. Schiek, Y. Xiong, *Chem. Eur. J.* **2002**, *8*, 5750-5760.

[12] A. Roux, R. Gillet, S. Huclier-Markai, L. Ehret-Sabatier, L. J. Charbonniere, A. M. Nonat, *Org. Biomol. Chem.* **2017**, *15*, 1475-1483.

[13] T. Price, S. Yap, R. Gillet, H. Savoie, L. Charbonnière, R. Boyle, A. Nonat, G. J. Stasiuk, *Chem. Eur. J.*, *doi.org/10.1002/chem.201905776*.

[14] aG. D. Hosken, R. D. Hancock, *J. Chem. Soc. Chem. Commun.* **1994**, 1363-1364; bR. Gillet, A. Roux, J. Brandel, S. Huclier-Markai, F. Camerel, O. Jeannin, A. M. Nonat, L. J. Charbonnière, *Inorg. Chem.* **2017**, *56*, 11738-11752.

[15] J. M. Berg, J. L. Tymoczko, L. Stryer, *Biochemistry*, 5th ed., New York: W. H. Freeman, **2002**.

[16] E. Molnár, B. Váradi, Z. Garda, R. Botár, F. K. Kálmán, É. Tóth, C. Platas-Iglesias, I. Tóth, E. Brücher, G. Tircsó, *Inorg. Chim. Acta* **2018**, *472*, 254-263.

[17] E. M. Gale, J. Zhu, P. Caravan, *J. Am. Chem. Soc.* **2013**, *135*, 18600-18608.

[18] J. Maigut, R. Meier, A. Zahl, R. van Eldik, *J. Am. Chem. Soc.* **2008**, *130*, 14556-14569.

[19] G. A. Rolla, C. Platas-Iglesias, M. Botta, L. Tei, L. Helm, *Inorg. Chem.* **2013**, *52*, 3268-3279.

[20] A. Borel, L. Helm, A. E. Merbach, *Chem. Eur. J.* **2001**, *7*, 600-610.

[21] M. K. Islam, S. Kim, H.-K. Kim, S. Park, G.-H. Lee, H. J. Kang, J.-C. Jung, J.-S. Park, T.-J. Kim, Y. Chang, *J. Med. Chem.* **2017**, *60*, 2993-3001.

[22] aJ. Wang, H. Wang, I. A. Ramsay, D. J. Erstad, B. C. Fuchs, K. K. Tanabe, P. Caravan, E. M. Gale, *J. Med. Chem.* **2018**, *61*, 8811-8824; bF. La Cava, A. Fringuello Mingo, L. Miragoli, E. Terreno, E. Cappelletti, L. Lattuada, L. Poggi, S. Colombo Serra, *ChemMedChem* **2018**, *13*, 824-834.

Entry for the Table of Contents

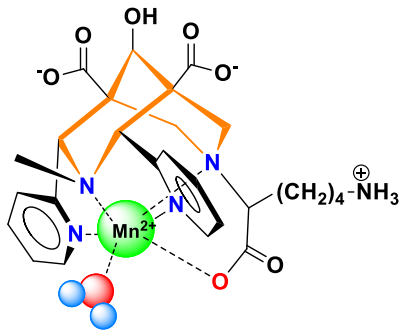

The 2,4-pyridyl-disubstituted bispidol ligand L_1 is a promising structural entry for the development of Mn-based imaging agents. Thanks to its preorganized, rigid structure, it provides exceptional inertness to the Mn^{2+} complex. MnL_1 is monohydrated, has good relaxation efficiency for MRI applications and undergoes rapid renal clearance when injected to mice. The ^{52}Mn-labeled radiocomplex could be obtained and was stable in biological media.